The Cytomechanics of Axonal Elongation and Retraction

Timothy J. Dennerll, Phillip Lamoureux, Robert E. Buxbaum, and Steven R. Heidemann

Department of Physiology, Michigan State University, East Lansing, Michigan 48824-1101

Abstract. Neurites of PC12 and chick dorsal root ganglion neurons behave as viscoelastic solids in response to applied forces. This passive behavior can be modeled with three mechanical elements; a relatively stiff, undamped spring in series with a Voight element composed of a less stiff spring in parallel with a dashpot. In response to applied tensions >100 microdynes, PC12 cells show lengthening behavior distinct from and in addition to the passive viscoelastic response. We interpret this as "towed growth" (Bray, D. 1984. *Dev. Biol.* 102:379–389) because the neurites can become twice as long without obvious thinning of the neurite and because in two cases neurite tensions fell below original rest tensions, a result that cannot be obtained with passive viscoelastic elements. The rate of towed growth showed a linear dependence of growth rate with applied tensions in 8 of 12 PC12 neurites exposed to applied tension >100 microdynes. Both PC12 and chick sensory neurons showed evidence of retraction when neurite tensions were suddenly diminished. This response was measured as tension recovery after slackening in chick sensory neurites. In 62% of the cases, tension recovery exceeded and sometimes doubled the preexperimental steady-state tension. Our data indicate that this response is active tension generation by the neurite shaft. We conclude that neurite length is regulated by axial tension in both elongation and retraction. Our data suggest a three-way controller: above some tension set point, the neurite is stimulated to elongate. Below some different, lower tension threshold the neurite is stimulated to retract. Between these two tension thresholds, the neurite responds passively as a viscoelastic solid.

NEURONAL shape and the complex pattern of connections in the nervous system depend on both progressive and regressive processes—e.g., axonal elongation and axonal elimination (Cowan et al., 1984; Purves and Lichtman, 1985). Axonal elongation appears to be regulated by mechanical tension. The last, "towing" phase of axonal elongation was long thought to be dependent upon tension caused by the migration of the neuron's target cell (Weiss, 1941). Bray (1984) confirmed this by eliciting ultrastructurally normal axonal elongation by experimentally applied tension. Recently, we showed that advancing chick sensory growth cones pull on their neurite shafts which grow from this tension (Lamoureux et al., 1989). Thus, the earlier, growth cone–mediated, elongation phases of "pioneering" and "application" (Weiss, 1941) also seem at least partly regulated by mechanical tension, as proposed originally by Bray (1982). In some tissues, the growth process overproduces synaptic connections, and axonal elimination subsequently occurs to produce the adult synaptic pattern (Purves and Lichtman, 1980). In the best studied system, polyneural innervation of skeletal muscle, axonal elimination occurs by axonal retraction not degeneration (Korneliussen and Jansen, 1976; Bixby, 1981; Riley, 1981; Morrison-Graham, 1983). This indicates that axonal elimination also depends upon cytomechanics since retraction must involve some force, presumably axonal tension, to withdraw the supernumerary processes. Campenot (1985) experimentally stimulated both neurite elongation and retraction of cultured rat sympathetic neurons by the addition or subtraction of nerve growth factor to different regions of the cells. The movement of cell body masses in response to neurite elongation and retraction suggested that both were regulated by mechanical tension.

To better understand the role of mechanical force in neuronal shape and growth, we have undertaken a quantitative investigation of the cytomechanics of PC12 cells and chick sensory neurons. Our results indicate that neurons are sensitive to the continuum of neurite tensions, with nerve fiber length regulated in part by those tensions.

Materials and Methods

Vector Analysis of Axial Force in PC12 Neurites

PC12 cells were cultured as previously described (Joshi et al., 1985). Neurite rest tensions and spring constants were measured by short-duration distensions as described by Dennerll et al. (1988). Using a modification of this method, the neurite was subsequently exposed to a long-duration distension (Fig. 1). Specifically, an initial rapid deflection of the calibrated force needle orthogonal to the neurite center was followed by 25–85-min periods during which the micromanipulator was undisturbed to allow for neurite lengthening (creep) and stress relaxation of the needle. A trial was ended by lifting the force needle and thereby releasing the neurite. As a control for ambiguous sources of neurite extension, trials were analyzed only if the growth cone–to–cell body distance changed <5%: i.e., neither the growth cone nor the cell body moved. Indeed, evidence that the cells were healthy and unaffected by the micromanipulations were those cases in which the growth

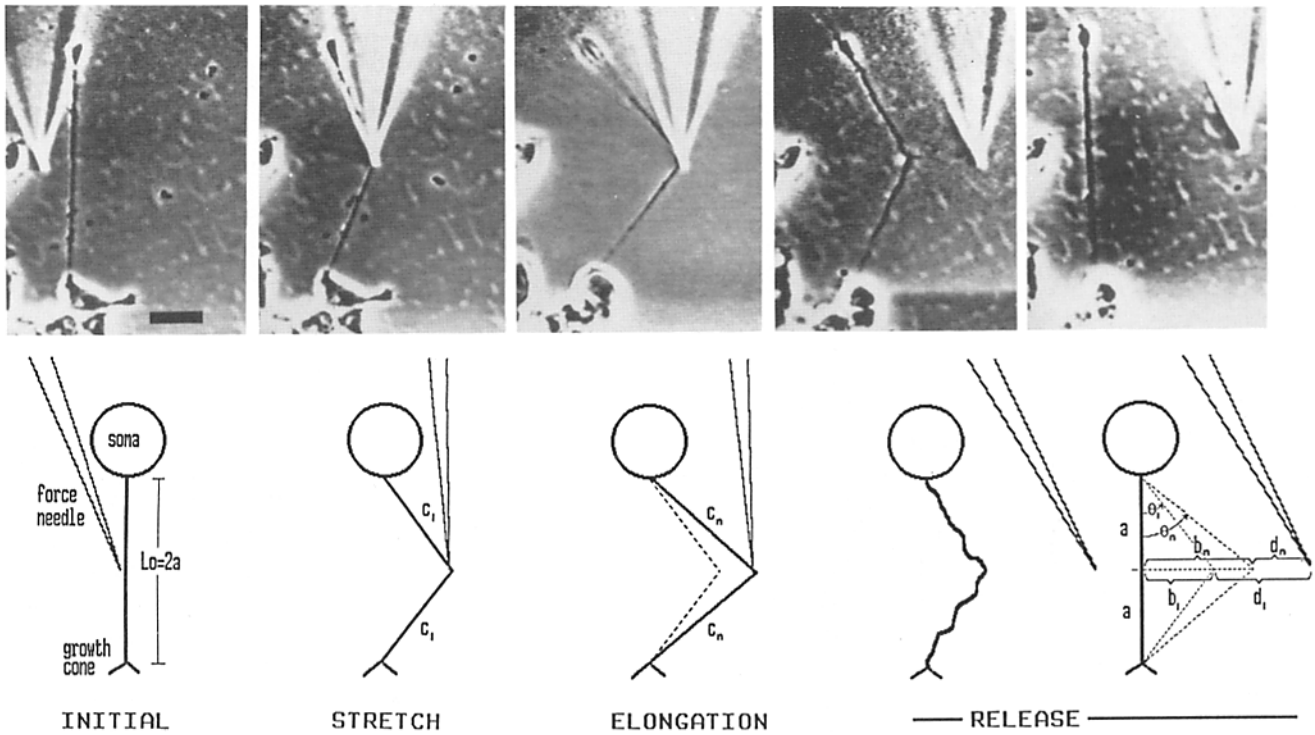

Figure 1. Lateral displacement method for measurement of PC12 tension and length changes. A calibrated glass needle is used to distend the neurite laterally at the neurite center, and the micromanipulator position is then held. Over time the neurite lengthens. Release of the needle allows for recovery of the neurite distension and for the needle to assume its zero force position for the applied micromanipulator movement. From the video record of the experiment, a measurement is taken of rest length (L_o) and, at 1–2-min intervals, of neurite lateral displacements (b_1, b_2. . .b_n) and the corresponding needle deflections (d_1. . .d_n). From these measured values at each time point, distended neurite lengths are determined by trigonometry and axial neurite tensions by vector algebra as described by Dennerll et al. (1988). Bar, 30 μm.

cone advanced significantly during the micromanipulation, causing the experiment to be discarded. In the few cases in which more than one neurite from a cell was examined, the first neurite remained normal and undamaged throughout the subsequent period of manipulation on the sister neurite. From the video record of these long-duration distensions, measurements of orthogonal neurite distension (*b*) and corresponding needle deflection from equilibrium (*d*) were taken at intervals of 1–2 min. These were used to calculate time records of neurite axial tensions and distended lengths using the vector analysis and trigonometric method described previously (Dennerll et al., 1988). In some experiments, a stock solution of taxol in DMSO (a gift of Dr. Mathew Suffness, Developmental Therapeutics Program of the National Cancer Institute, Bethesda, MD) was added to the culture media to achieve a final concentration of 1 μM taxol and 0.1% DMSO. Long-duration distensions were begun 5–10 min after addition of the drug.

Direct Axial Force Measurements in Chick Dorsal Root Ganglion (DRG)[1] Neurites

Embryonic chick DRG neurons were grown as previously described (Baas and Heidemann, 1986). As shown in Fig. 2, DRG neurites were distended by pulling axially with the calibrated needle attached directly to the growth cone. Side deflection, as for PC12, frequently detached the growth cone, making distension impossible. A glass needle calibrated for its bending modulus (*Cal*) as described (Dennerll et al., 1988) was treated by immersion in 0.1% polylysine in PBS, then in 1 mg/ml collagen type IV (Sigma Chemical Co., St. Louis, MO) in PBS, and then in 20 μg/ml laminin (Collaborative Research, Lexington, MA) in L-15 medium; each immersion was for 30 min at room temperature. This sequence of immersion was repeated with air drying between each step and the needle was stored. Immediately before use, the needle was treated with laminin as above. The force-calibrated needle was mounted in a single micromanipulator with its tip a short distance (*r*) from a stiffer reference needle. To maintain cells at physiologic temperatures and to minimize thermal changes in micromanipulator position, the entire laboratory room was maintained at 37°C. Neurites 80–200 μm long were manipulated to get the growth cone attached to the calibrated needle without detaching the cell body from the dish (Fig. 2). After growth cone attachment, the needles were raised slightly so that only the cell body remained attached to the substratum and so that the neurite was at its original length. To obtain stable growth cone attachments and as a control for the effect of needle attachment, the neurite was not distended or slackened by micromanipulation for ~1 h. That is, before all DRG experiments, the neurite was allowed to reach an apparent plateau length and tension. For long-duration distension experiments, the attached neurite terminal was rapidly drawn away distally, and this micromanipulator position was held for periods of 30–215 min. From the video record of this distension, measurements were taken at intervals of 1–4 min of neurite length and needle gap distance ($d + r$). Neurite axial tension was calculated for each measurement as the product of the calibrated needle deflection distance (d) and its force calibration constant (Cal). For slackening experiments, the attached neurite terminal was rapidly micromanipulated proximally (backed up), and this micromanipulator position was held for periods of 25–160 min. Time records of neurite lengths and tensions were obtained as above. Because the growth cone was attached to the needle, it was not possible to ascertain the growth of the neurite after manipulation. However, several bouts of similar manipulations with the needle attached to the cell body do not cause any damage to the growth mechanism of the neurite (Lamoureux et al., 1989).

Determination of Neurite Mechanical Constants and Computer Simulation of Neurite Viscoelastic Distension Behavior

We have modeled neurite distension behavior with a system of two springs and a dashpot (Fig. 5). The values for these three mechanical constants were determined from the distension data for each neurite modeled. According

1. *Abbreviation used in this paper*: DRG, dorsal root ganglion.

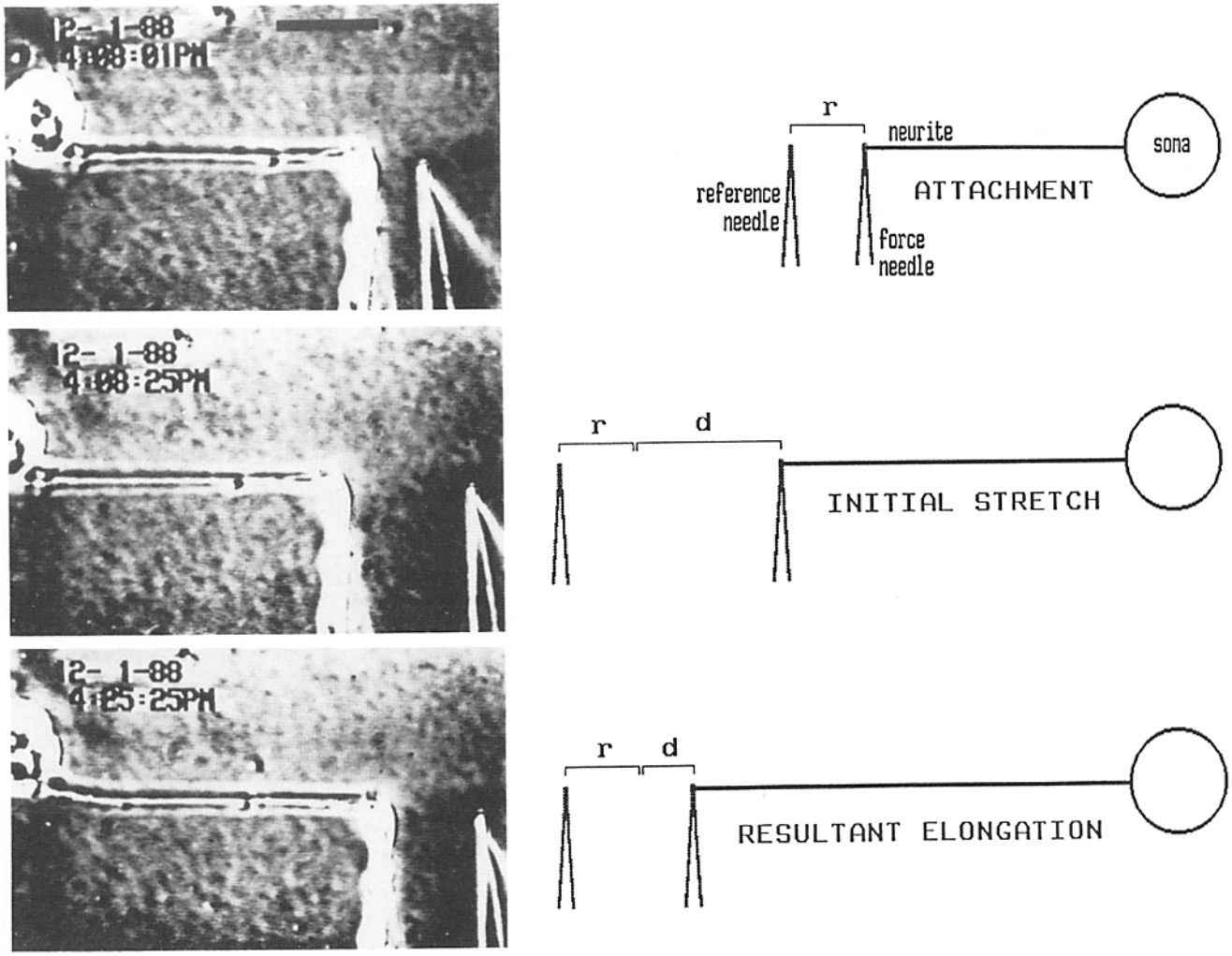

Figure 2. Direct axial method for measurement of chick DRG neurite tension and length changes. A growth cone is attached to a calibrated glass needle that is mounted a short reference distance (r) from a stiff, unloaded reference needle that moves only with movement of the micromanipulator system. A single, axial, distal movement of the needles is applied to the neurite and held for periods of 30–215 min. From a videotape record of the experiment measurements are made of the reference distance, r, and, at intervals of 1–4 min, of neurite length and needle gap distance ($d+r$). These values are used to determine for each time point neurite axial tension ($d \times$ calibration factor of needle, where d = gap distance $- r$) and changes in neurite length. The sole modification of this technique for measurement of tension generation by the neurite shaft is that a single, axial, proximal micromanipulator movement is made to initially slacken the neurite. Bar, 40 μm.

to classical mechanical concepts, the Voight element response is "sluggish," its motion is effectively nil during transient changes in system tension. However, the free spring (modulus k_1 in microdynes per micrometer) does respond immediately and is therefore the only mechanical element to move during short-duration (1–2 s) distensions. The value for k_1 was therefore obtained from the slope of a plot of neurite tension against neurite length change from a series of short-duration distensions (Dennerll et al., 1988). Similarly, an overall neurite elastic modulus, K_{nrt}, was obtained by dividing the net change in neurite tension by the corresponding change in neurite length using steady-state values ("plateau values") at the beginning and end of the long-duration distension experiments. Because we are comparing two steady-state values, the dashpot has a negligible effect and the following relation holds: $1/K_{nrt} = 1/k_1 + 1/k_2$. The value for the Voight element spring (modulus k_2) is thus (rearranging this equation) $k_2 = 1/([1/K_{nrt}] - [1/k_1])$. Because of noise in the long-duration data, dashpot (viscosity) constant (H) was calculated by matching the experimental data to that predicted from a numerical solution (described below) of the relevant differential equation for various test values of H.

The differential equation relating force to distension for the proposed model (Fig. 5) is easily solved for an axial step change in force once k_1, k_2, H, Cal, and the initial and applied forces are known. A computer program was developed that allowed us to enter these values as well as a time interval between calculations and a total time duration for the experiment. The program then simulated the neurite lengths and axial tensions as a function of distension time. All but the value of H was known from the experimental data. We arrived at a value for H by interactively minimizing the differences between predicted and experimental behaviors. For orthogonal pulling experiments on PC12, the procedure for simulating neurite distension was similar but more complex since the relevant differential equation could not be solved analytically (because of sin θ terms). Thus, the computer first solved the differential equation numerically using a version of Euler's method and then printed the results, as before, for comparison with the experimental data. Please contact the authors for a copy of these programs (written in APL) and their documentation.

Results

Viscoelastic Response to Neurite Distension

In 20 trials on 13 PC12 cells, neurites were observed for

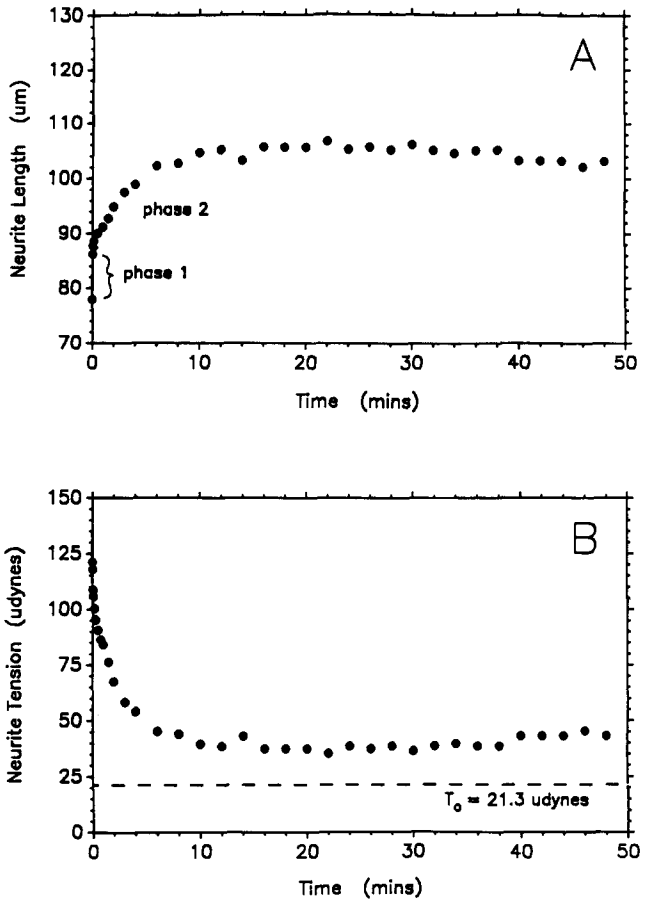

Figure 3. Response of PC12 neurites to lateral displacement as in Fig. 1. (*A*) Change in neurite length (neurite creep) with time after a single distension. (*B*) Change in neurite tension (stress relaxation) with time after a single distension. Typical of all applied tensions to PC12 <100 microdynes, an initial rapid change in length/tension (phase 1) is followed by a damped approach (phase 2) to new plateau values.

25–85 min after a single, orthogonal needle displacement (see Fig. 1 and Materials and Methods). In eight trials, initial applied forces were ≤100 microdynes; under these conditions, we observed a two-phase viscoelastic lengthening response and stress relaxation (Fig. 3). A rapid increase in neurite length and tension (phase 1) was followed by a slow, damped approach (phase 2) to plateau values where length increased and tension decreased. For these experiments, as seen in Fig. 3, plots of neurite tension over time mirror plots of neurite length because neurite length and needle deflection are directly coupled.

Recovery from these distensions after release was rapid; the neurite typically became visibly straight and normal in appearance within 1 min. In all eight trials, a series of short-duration distensions were made 1–5 min before and 1–10 min after a long-duration distension to determine if it had an effect on the neurite's elastic properties. After long-duration distensions, rest tensions averaged 115 ± 27% (SEM) and spring constants averaged 170 ± 18% of initial values.

In 24 trials on 15 DRG neurons, neurites were observed for 30–215 min after a single axial pull from the distal end (see Fig. 2 and Materials and Methods). Like PC12, these neurites also exhibited a two-phase viscoelastic lengthening and tension response (Fig. 4). However, unlike PC12, this reponse was not limited to applied forces <100 microdynes.

Mechanical Model for Passive Viscoelastic Behavior of Neurites

These data indicate that both PC12 and DRG neurites respond to long-duration distension as viscoelastic solids. By this we mean that the deformation response of neurites to applied force has both fluid- and solid-like properties, resulting in a final equilibrium between force and deformation characteristic of solids. We have modeled this behavior with a simple combination of three classical mechanical elements (Fig. 5 *A*): a relatively stiff spring (spring constant k_1) in series with a Voight element, which consists of a (less stiff) spring (k_2) in parallel with a dashpot (dashpot constant H). The constants describing these three mechanical elements were calculated as described in Materials and Methods for two PC12 and two DRG neurites. Essentially, the spring constants were determined analytically from the experimental data, and the dashpot constant was chosen by matching of mechanical model behavior to experimental observations.

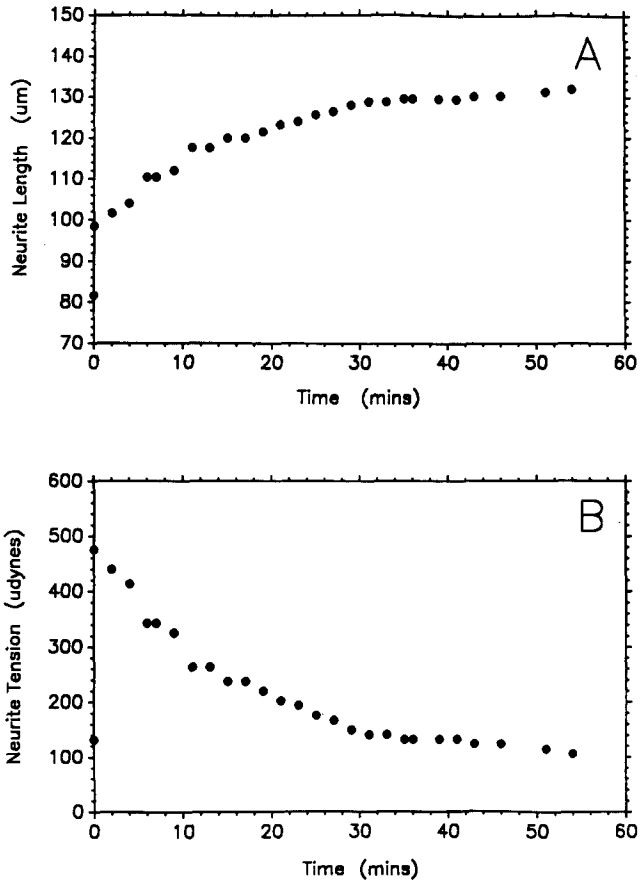

Figure 4. Response of chick DRG neurite to axial stretch as in Fig. 2. (*A*) Change in neurite length (neurite creep) with time after a single distension. (*B*) Change in neurite tension (stress relaxation) with time after a single distension. Chick sensory neurites, like PC12, also respond to long-duration distensions with an initial rapid change in length/tension (phase 1) followed by a damped approach (phase 2) to new plateau values.

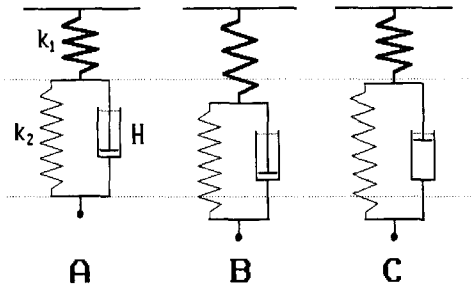

Figure 5. Mechanical model for the passive viscoelastic response of neurites to long-duration distensions and their behavior. (*A*) The combination of a relatively stiff, undamped spring (spring 1; constant k_1) in series with a Voight element (spring 2; constant k_2) in parallel with a dashpot (dashpot constant H) can be used to describe the cytomechanical response of neurites shown in Figs. 3 and 4. (*A–C*) The behavior of the mechanical system to a step increase in its length. *A* shows the system before distension at equilibrium (force balance). (*B*) Immediately after distension, tension rises because of the instantaneous response of spring 1. (*C*) At later times the dashpot flows allowing spring 2 to elongate and spring 1 to shorten, thus, lowering the measured tension until the system comes into equilibrium with equal tension in both springs. This final tension will be slightly higher than the initial tension at *A*, shown by the extension of spring 1 relative to the upper dotted line. At any given time, the measurable system tension will be proportional to the extension of spring 1.

As shown in Fig. 6, these simulations closely match the observed behavior for neurites of both cell types. A feel for the contribution of individual model elements is gained by simulating the distension behavior of a family of hypothetical neurites that vary only in one mechanical element; this is done in Fig. 7.

Tension Induced Phase 3 "Growth"

In 9 of the total 20 trials on PC12 neurons, neurites were subjected to initial applied forces >100 microdynes; these neurites then exhibited a three-phase lengthening response. Phases 1 and 2 (discussed above) were followed by a third period where elongation and tension decrease either failed to plateau before the trial ended or plateaued only after neurite axial tension fell below 50–100 microdynes (Fig. 8). In two cases, neurites were exposed to both a low and high initial applied force. A clear qualitative difference was observed between the low-force (<100 microdynes) two-phase response and the high-force (>100 microdynes) three-phase response for both neurites, as seen in Fig. 9. In an additional two cases, final neurite tensions near the end of the distension were approximately half of the initial rest tensions, a result that cannot be accounted for by passive viscoelastic behavior.

After release, neurites that exhibited a three-phase elongation typically lay flaccid and sinusoidal on the dish for up to several minutes; they were obviously longer but not thinner as a result of experimentally applied forces (see Fig. 1). Within 5–15 min, these neurites shortened and finally straightened between the growth cone and cell body attachments to the dish. In eight trials, when a series of short-duration distensions were successfully made both before and after recovery from a long-duration distension, final rest tensions averaged 93 ± 16% and final spring constants averaged 93 ± 22% of initial values.

For purposes of analysis, we defined phase 3 elongation as beginning 10 min after the initial application of experimental tension. This criterion was our best attempt to compromise two opposing criteria, excluding the phase 2 behavior that dominates the early response and retaining enough data for analysis. Fig. 10 plots average phase 3 elongation rate against initial applied force for each of the 20 long-duration distension trials. Fig. 10 suggests a threshold value of ~100 microdynes to achieve a positive phase 3 elongation rate and also a roughly linear dependence of elongation rate on applied force >100 microdynes. However, in 3 out of 20 trials on PC12 neurons, the neurites responded to initial applied forces >100 microdynes by exhibiting a two-phase lengthening response (near zero phase 3 elongation rate) and rapid (<1 min) recovery typical of the behaviors observed for initial applied forces <100 microdynes (Fig. 10).

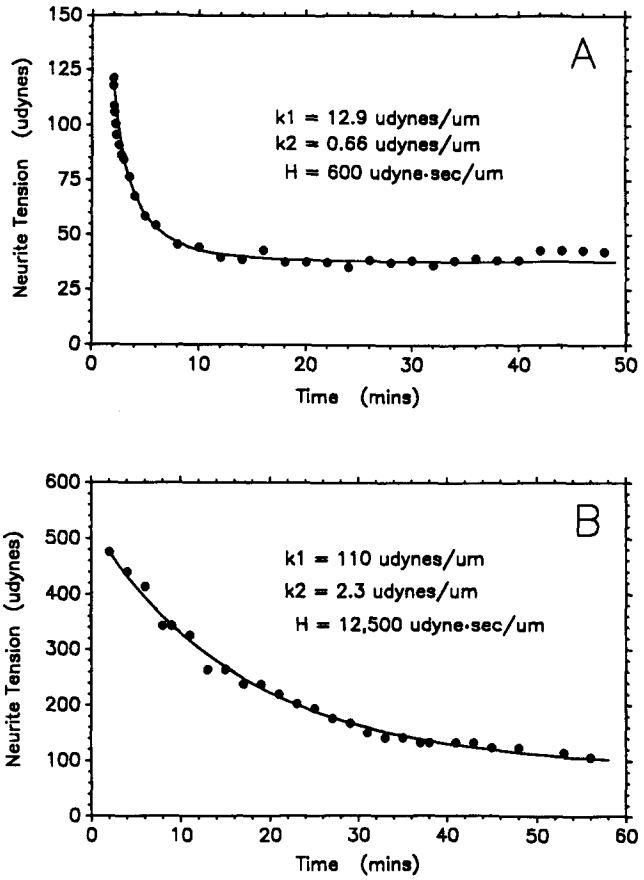

Figure 6. Comparison of neurite distension data with the predicted behavior of the mechanical model shown in Fig. 5. (*A*) Experimental data (*solid circles*) from a PC12 neurite and (*solid line*) the predicted viscoelastic response of the three-element mechanical model having the moduli given in the box to the same (as experimental) initial applied force. (*B*) Experimental data (*solid circles*) from a DRG neurite and (*solid line*) the predicted viscoelastic response of the three-element mechanical model having the moduli given within the box to the same initial applied force. As described in the text, the spring constants for the mechanical model were derived analytically from the experimental data, while the dashpot constant was fitted by iterations of the computer program.

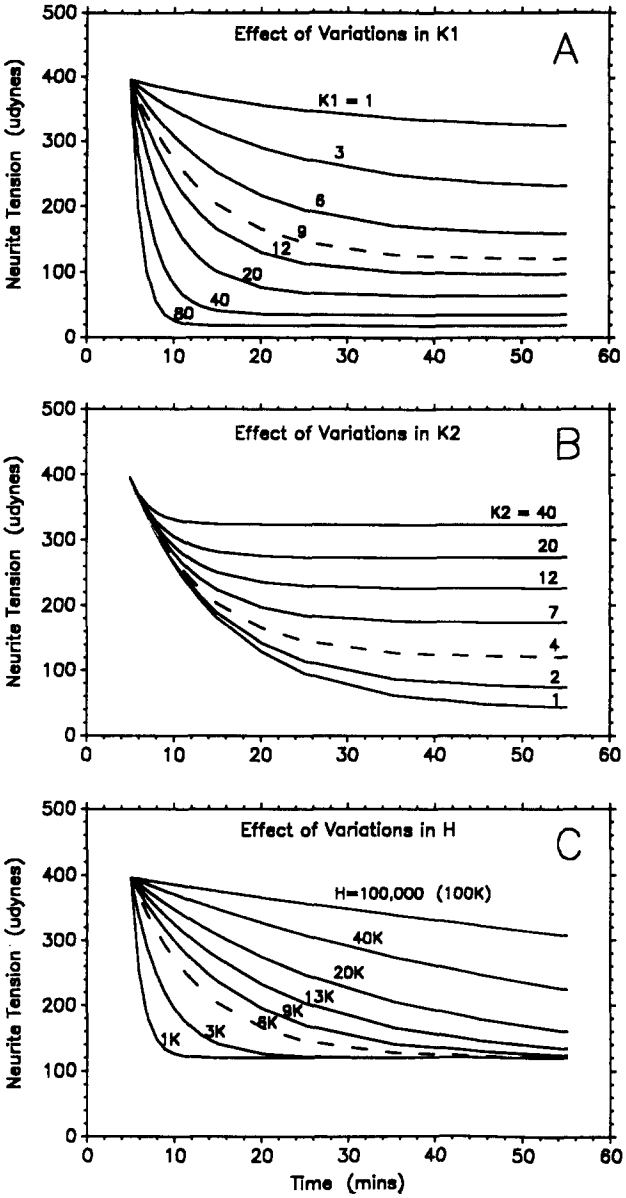

Figure 7. The effect of changes in spring and dashpot constants on the behavior of the three-element mechanical model (Fig. 5 *A*) to an initial applied force of 400 microdynes. In all panels, predicted axial tensions are plotted against time. For each panel, two moduli are held constant and the third is systematically varied. (*A*) The constant (k_1) of the stiff, undamped spring is varied, while k_2 = 4 microdynes/μm and H = 6,000 microdynes · s/μm. As spring 1 is stiffened, its initial extension to accommodate 400 microdynes decreases. Subsequent accomodation of spring 1 tension through the extension of spring 2 causes spring 1 to shorten. This shortening of spring 1 dissipates progressively more force as its spring constant increases. This causes the displayed progressive decline in the tension plateau value as spring 1 is stiffened. (*B*) The constant of spring 2 (k_2) is varied, while k_1 = 9 microdynes/μm and H = 6,000 microdynes · s/μm. The initial extension of spring 1 to accommodate 400 microdynes is constant throughout. As spring 2 is stiffened, it elongates progressively less to subsequently accommodate the tension, causing a progressive decrease in the shortening of spring 1 with time. This is responsible for the increase in plateau tension levels with increase in K_2. (*C*) The dashpot constant is varied, while k_1 = 9 and k_2 = 4 microdynes/μm. The dashpot does not effect the plateau value of tension, only the time of approach to plateau. If the lines for the larger dashpot constants were extended for sufficiently long periods, all curves would reach the same plateau. As the viscosity of the dashpot declines, the force causes more rapid flow allowing springs 1 and 2 to reach equilibrium more quickly. The dotted line in each panel shows identical behavior for the case k_1 = 9 microdynes/μm, k_2 = 4 microdynes/μm, and H = 6,000 microdynes · s/μm.

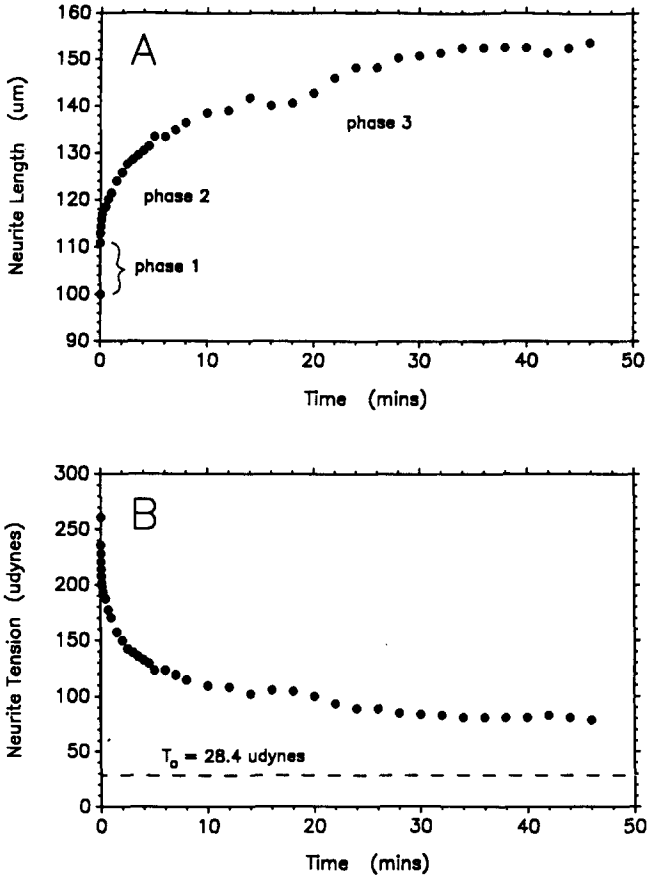

Figure 8. Response of a PC12 neurite to a long-duration distension with initial applied force >100 microdynes. (*A*) Neurite length as a function of time after an initial applied force of 233 microdynes. (*B*) Neurite tension as a function of time after the same initial force application. As shown here, 10 of 12 PC12 neurites responded to initial applied force >100 microdynes with a third phase of elongation that continued for as long as the neurite was observed or until neurite tension fell below 50–100 microdynes.

Taxol Inhibition of Phase 3 Elongation

In five trials on five PC12 neurons, neurites were exposed to initial applied tensions >100 microdynes in the presence of 1 μM taxol, a potent stimulator of microtubule assembly (Schiff et al., 1979). In these neurites, phase 3 elongation was completely eliminated with little or no qualitative effect on either phase 1 or 2 (Fig. 11). In these experiments, the neurite recovers rapidly after release from the high initial applied force, typically becoming straight and normal in appearance within 2 min. In three out of five of these taxol trials, we were able to perform a series of short-duration distensions both before and after the long-duration distension. The values for recovered rest tensions and spring constants

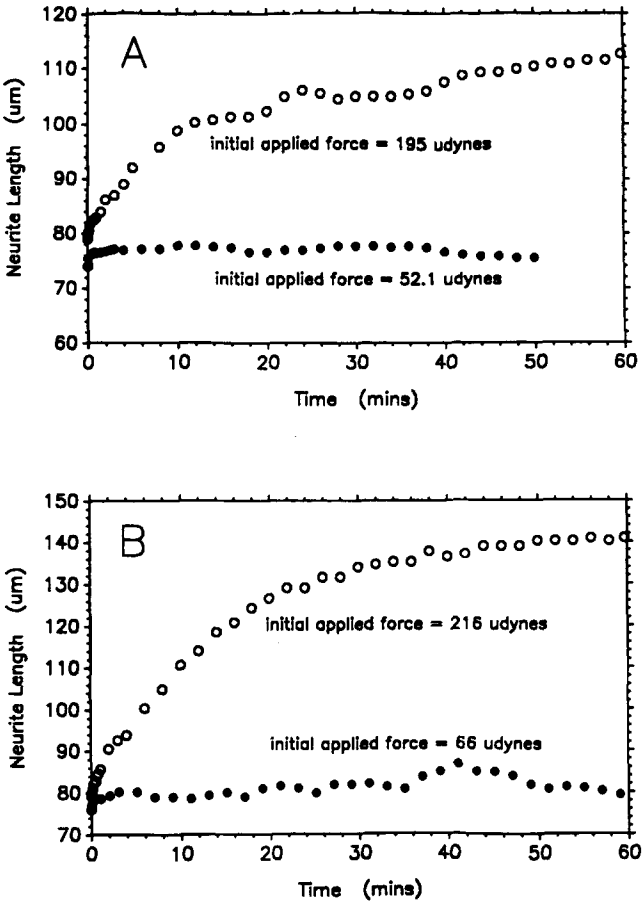

Figure 9. Response of two PC12 neurites to applied forces greater and less than 100 microdynes. Plots of neurite length with time are shown for two neurites, each subjected to two force levels as labeled on the curves. Both neurites showed phase 3 elongation only in response to initial applied forces >100 microdynes.

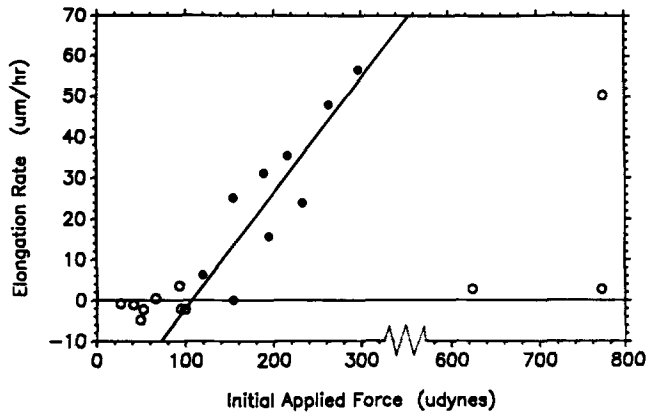

Figure 10. Phase 3 elongation rate of PC12 neurites as a function of initial applied tension. Each circle is the rate of neurite elongation for the period beginning 10 min after the initial application of force (phase 3 elongation) plotted against the value of the initial applied tension. All eight neurites initially subjected to applied force <100 microdynes showed elongation rates near zero. 9 of 12 neurites (*solid circles*) subjected to applied force >100 microdynes showed a linear correlation of phase 3 elongation rate with applied force. Only solid circles were used in plotting the least squares fit linear regression line shown as a solid line. The remaining three neurites subjected to applied force >100 microdynes showed no correlation of elongation rate with applied force.

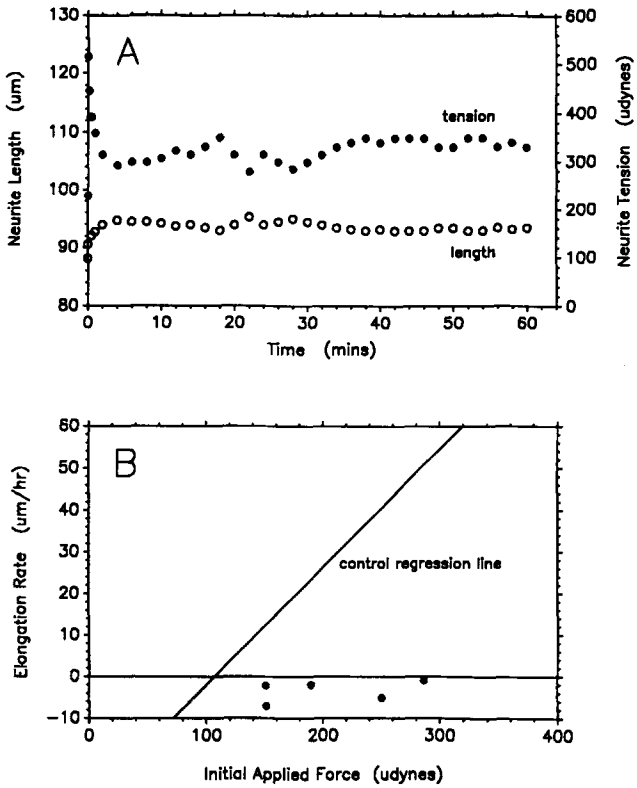

Figure 11. Response of PC12 neurites to applied forces >100 microdynes in the presence of taxol. (*A*) Neurite length and tension as a function of time for a single trial with an initial applied force of 287 microdynes in the presence of 1 μM taxol. As shown here, all such neurites responded with a two-phase viscoelastic response. (*B*) Phase 3 elongation rate as a function of initial applied force for neurites in the presence of 1 μM taxol. The regression line for unpoisoned neurites as in Fig. 10 is reproduced here for comparison. No taxol-poisoned neurites showed phase 3 elongation.

were higher than initial values, similar to the unpoisoned, two-phase recoveries; final rest tensions averaged 185 ± 34% and final spring constants averaged 148 ± 45% of initial values.

Redevelopment of Neurite Tension after Slackening

We previously reported that DRG neurites that were slackened appeared to redevelop tension (Lamoureux et al., 1989). The slow recovery of PC12 neurites from phase 3 elongation also suggested to us that the neurite might be actively producing tension to shorten. We investigated this possibility in chick DRG neurons in which the force measurement technique allows quantitative observations of shortening. We observed the effect of a sudden decrease in DRG neurite tension by measuring neurite tensions after a back up micromanipulation that slackened the neurite (see Materials and Methods). In all 26 trials on 15 DRG neurons, there was a clear redevelopment of tension after slackening (Fig. 12). In 10 trials, neurites redeveloped tension to a plateau below the initial, pre-back up tension to an average of 70% of the initial tension (Fig. 12 *A*). However, in 16 trials, the neurite achieved tensions higher than initial values with final tensions averaging 152% of the initial tension (Fig. 12 *B*). In two of five neurites that underwent two consecutive back ups,

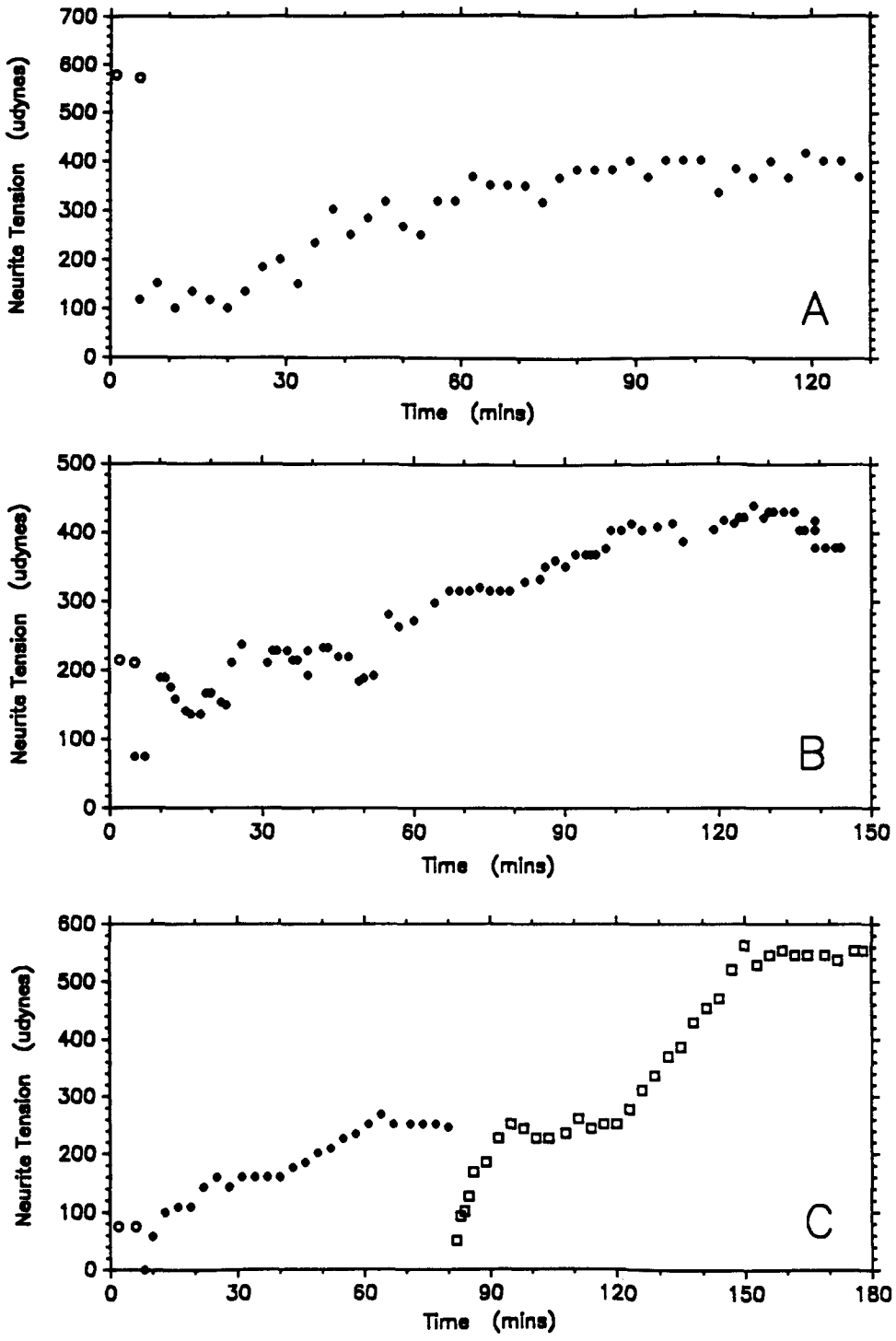

Figure 12. Response of chick DRG neurites to slackening. Neurite tension with time after a sudden decline in neurite tension. For all panels the open circles represent the preexperimental plateau as the last two time points before backing up the micromanipulator. (*A*) The response of a neurite that did not recover to the preexperimental tension level. This result was obtained in 10 out of 26 trials. (*B*) The response of a neurite that developed tension to a level greater than the preexperimental equilibrium. This result which cannot be obtained with passive springs or dashpots was obtained in 16 out of 26 trials. (*C*) One of two neurites that overshot the previous plateau tension value after both of two consecutive slackenings. This result cannot be obtained from passive springs or dashpots.

tension recovered above its previous apparent plateau both times (Fig. 12 *C*). There was a tendency for a given neurite to behave similarly in repeated trials. For example, neurite 15 consistently failed to recover to initial tension values in three trials, while neurite 7 more than doubled its initial tension values in both of its trials. No other factor analyzed thus far—including previous back up treatment, initial neurite length, initial tension, or relative or absolute amount of tension drop—correlated with either the absolute or relative amount of tension recovery.

Our previous results suggested that the neurite shaft developed tension only after slackening (Lamoureux et al., 1989). To confirm this and as a control for the effect on needle tension of needle attachment to the growth cone, the mechanical response of DRG neurites to needle attachment in the absence of distension or slackening was assessed for 40–75 min. In all nine trials on nine DRG neurons, lasting from 40–75 min, neurite tension remained relatively steady as shown for three representative neurites in Fig. 13.

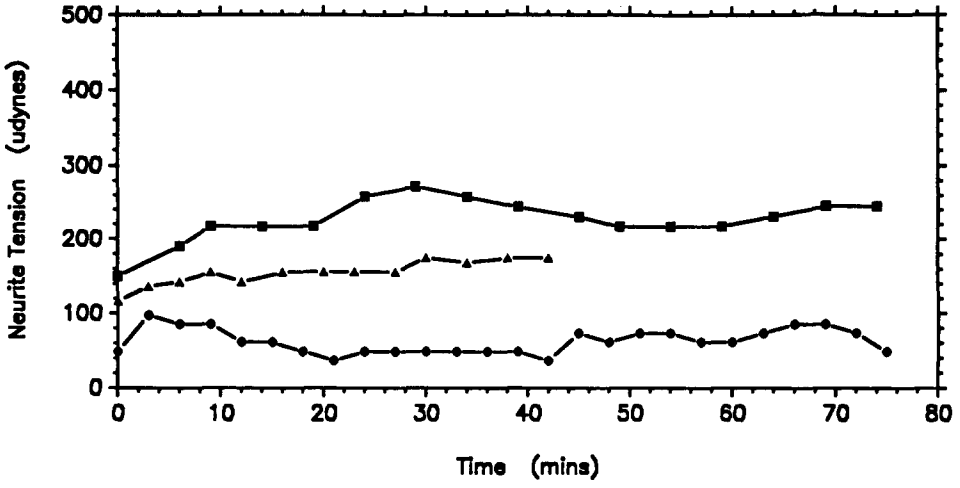

Figure 13. Response of chick DRG neurites to micromanipulation without stretching or slackening. Neurite tension as a function of time for three representative neurites that were attached to calibrated needles and allowed to incubate at their preexperimental length without experimentally induced changes in neurite tension. As shown here, all nine such neurites maintained fairly steady neurite tensions.

Discussion

We found that neurites respond passively to force by deforming as viscoelastic solids, as previously reported for other cell types (Mitchison and Swann, 1954; Hiramoto, 1963, 1970; Pasternak and Elson, 1985). Consistent with viscoelastic solid behavior, we observed two-phase elongation/stress relaxation behavior leading to new, steady-state values for both PC12 and chick DRG neurites using two different measurement techniques. Also, consistent with a passive elastic response was the rapid recovery from these biphasic elongations; neurites returned to original linear morphology within 1 min after release. Neurite behavior matched closely the predicted behavior of the three-element mechanical mode of a viscoelastic solid shown in Fig. 5, as shown by computer simulation. In addition to confirming the validity of this model, the computer simulation program also provided us with a better understanding of the possible response changes that could occur through qualitative differences in spring and dashpot constants (Fig. 7). We hope that this quantitative approach will, in the future, permit a better understanding of the role of particular cytoskeletal elements in determining the mechanical properties of the cell. For the present, however, we can provide only a very limited biological interpretation for the specific values of the spring and dashpot constants of the mechanical model. DRG neurons in all cases proved to be mechanically stiffer than PC12 neurons; generally both spring constants of DRG neurites were 5–10 times greater and dashpot constants were some 10–20 times greater than those of PC12 neurites. We speculate that this may be due in part to neurofilaments, which are common in DRG neurites but are not a significant feature of PC12 ultrastructure (Luckinbill-Edds et al., 1979; Heidemann et al., 1985; Jacobs and Stevens, 1986). Earlier work with cytochalasin D (Dennerll et al., 1988) points to a strong association of the undamped spring (k_1) with a neurite actin network, presumably the cortical actin network beneath the axolemma (Hirokawa, 1982; Schnapp and Reese, 1982). Unfortunately, most anticytoskeletal drugs have side effects—e.g., causing loss of growth cone adhesion and/or neurite retraction—that prohibit a clear interpretation of the cytoskeletal basis of these constants.

PC12 neurites exposed to initial applied forces of >100 microdynes showed an additional third phase of elongation (Fig. 8) that we interpret as towed neurite growth, entirely similar to that previously reported by Bray (1984) in response to experimentally applied tension. This interpretation is supported by the observation that neurite lengths increased up to 218% of initial length during distension without observable changes in diameter or obvious damage. Also, in two trials, final plateau neurite tensions were below initial rest tensions. This result cannot be obtained with any combination of passive springs and dashpots, but is consistent with tension dissipation through mass addition. These neurites also showed recovery behavior that was distinct from two-phase recovery, requiring significantly longer times to recover to original linear morphology. In some respects, phase 3 elongation is characteristic of dashpot behavior. Thus, in Fig. 14 we model total neurite response by the addition of a special "growth dashpot" in series with the previous model in Fig. 5 *A*. This growth dashpot elongates in a manner similar to flow, albeit by the living mechanism of mass addition. Growth cannot be controlled by varying the values k_1, k_2, and H because growth is inelastic; a given neurite length is not associated with a given force. Putative growth from this element appears to occur above a tension set point of ~100 microdynes in PC12. Above this tension load, towed growth occurred in 8 out of 12 neurites with a linear dependence of

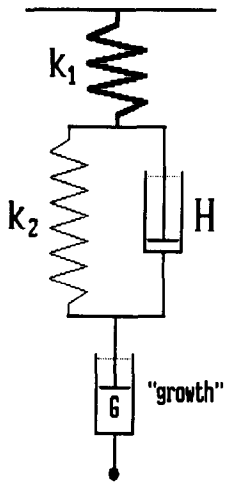

Figure 14. Mechanical model of PC12 neurite behavior including phase 3 elongation. An additional growth dashpot is added in series to the mechanical model shown in Fig. 5 *A*. Phase 3 elongation resembles the response of a dashpot to tension in dissipating the tension through elongation and in the linear relationship between applied tension and elongation rate. Insofar as we have interpreted phase 3 elongation to be growth, it is not surprising that phase 3 has some aspects that cannot be accounted for by any purely passive mechanical element; among these are the apparent dependence of phase 3 upon microtubule assembly and the change in elongation behavior above and below certain tension thresholds.

growth rate on applied force (Fig. 10). Below this level, all eight neurites showed near zero elongation rates. The existence of a set point is further supported by the different elongation behavior of two neurites that were subjected to initial applied forces both below and above 100 microdynes (Fig. 9). We investigated the role of microtubule assembly in phase 3 elongation by observing the effects of 1 μM taxol, a known stimulator of microtubule assembly on long-duration distensions above an initial applied force of 100 microdynes. While taxol treatment showed no effect on phase 1 or 2 elongation, the phase 3 elongation rate was strongly inhibited compared with the control (nondrugged) neurites (Fig. 11); i.e., taxol locks up the growth dashpot in Fig. 14. Our interpretation is that tension-induced growth is dependent upon microtubule assembly, as expected for neuronal growth in general (Mitchison and Kirschner, 1988). Taxol may be disrupting the normal microtubule assembly necessary for neurite growth in a manner similar to the reported taxol inhibition of growth cone–mediated growth (Letourneau and Ressler, 1984; Sinclair et al., 1988). This growth inhibition seems likely to be the result of tubulin dimer depletion but could also be due to a structural interference in the growth process caused by the addition of the "taxol microtubules."

Using the distension method here, a single pull allowed to relax over time, we were unable to distinguish in DRG neurites a third phase of elongation distinct from passive viscoelastic behavior. This is not surprising given their greater mechanical stiffness. DRG neurites require substantially longer times than PC12 to passively dissipate a strain, as can be seen by comparing Fig. 3 with Fig. 4. For typical experimental durations of 60–70 min, any distinct growth response would be hidden in the passive behavior. Also, the greater stiffness of DRG neurites dictated the use of stiffer needles that were moved shorter distances to apply a given force. Because a neurite cannot elongate further than the initial movement of the micromanipulator, DRG neurites had a very limited opportunity for continued phase 3 elongation. Various observations nevertheless suggest a tension threshold for DRG neurites as well. First, the neurite was held at a positive tension for ~1 h without elongation to obtain a preexperimental plateau value for tension. Also experiments in progress, in which DRG neurites are subjected to 1-h-long steps of constant force, suggest that these neurites, like PC12 neurites, respond differently to low and high applied tensions.

Chick DRG neurites are able to actively generate tension in response to decreases in applied force. When these neurites are slackened, they respond with a biphasic shortening and tension recovery that looks like the inverse of the two-phase response to distension discussed above (Fig. 12). The viscoelastic model shown in Fig. 5 *A* predicts passive tension recovery to slightly less than the initial preslackened value, demonstrated by a sequence that is the converse of the lengthening events in Fig. 5. An instantaneous shortening in length causes neurite tension to fall immediately as spring 1 shortens, but the response of the Voight element spring is delayed by the slowness of the dashpot response. Tension is thus "stored" transiently in the Voight element. As the dashpot flows out, this "reserve" tension equilibrates over the whole system causing the Voight element to shorten and spring 1 to elongate. The lower tensions predicted by this purely passive response were obtained experimentally only 38% of the time after a neurite shortening. In 62% of the trials tension recovery exceeded and sometimes even doubled initial values. In two neurites, this overshoot response was exhibited twice after each of two consecutive slackenings (Fig. 12 *C*). These latter results imply active tension generation by the neurite. Insofar as actin and myosin have repeatedly been localized to the neurite/axon cortex (Roisen et al., 1978; Kuczmarski and Rosenbaum, 1979; Bridgman and Daily, 1989), it seems likely that this tension generation is the result of some actomyosin mechanism. This tension generation was observed in this and in previous experiments (Lamoureux et al., 1989) to require the stimulus of neurite slackening. Experiments in which the neurite was attached to a needle but was not subsequently slackened failed to produce significant tension changes (Fig. 13).

We conclude that neurite/axon length is regulated by axial tension in both elongation and retraction, as previously suggested by Campenot (1985). More specifically, our data suggest a tension-sensitive, three-way control of neurite length (Fig. 15) via a reversible growth process—e.g., the growth dashpot of Fig. 14. Neurite tensions above some upper threshold value (set point) stimulate elongation, presumably involving cyoskeletal assembly. A tensile regulatory mechanism is not unexpected given the evidence for towed growth and a pulling growth cone (Weiss, 1941; Bray, 1982, 1984; Lamoureux et al., 1989). At some different, lower tension threshold (set point), neurites are stimulated to generate tension and thereby retract. Our data support Campenot's (1985) proposal that the tension generation and retraction response is the reverse of growth: e.g., in our model the growth dash-

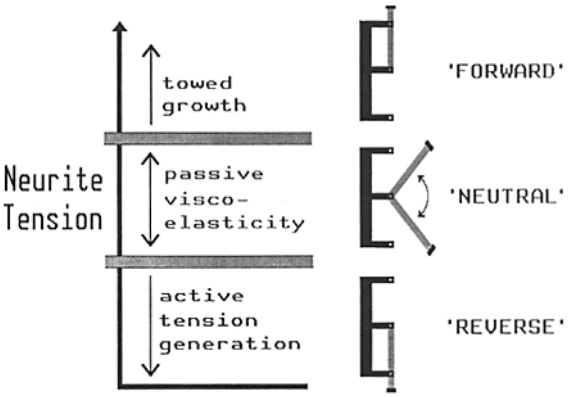

Figure 15. Diagrammatic representation of a proposed three-position control for tension regulation of neurite length. The figure on the left summarizes the response of neurites to changes in neurite tension, while the figures on the right put this response into the context of a familiar three-position control: a double-pole, double-throw electric switch. Our data for PC12 cells suggests that at neurite tensions above some threshold, towed growth (Weiss, 1941; Bray, 1984) occurs. In the context of the control of the growth dashpot pictured in Fig. 14, this reflects a switch in one of two oppositely acting positions causing the dashpot to elongate. At neurite tensions below a different, lower threshold, the neurite is stimulated to generate tension, shortening the neurite. The control is shown in the reverse position causing the dashpot to shorten. At neurite tensions between the two thresholds the neurite responds with passive viscoelastic behavior. That is, the growth dashpot is not engaged because the control is in neutral, not making contact with either pole.

pot (Fig. 14) shortens, generating tension and shortening the neurite. We presume that the tension generation we observed is responsible for the complete retraction into the cell body of the proximal portions of severed neurites of chick sensory or PC12 cell (Shaw and Bray, 1977; Wessells et al., 1978; Joshi et al., 1985; George et al., 1988). This is supported by the similarity in the time scale for retraction (Shaw and Bray, 1977; Wessells et al., 1978; George et al., 1988) and for tension generation of DRG neurites, both ~20–60 min. A similar mechanism may underlie the retraction of axons from the neuromuscular junction (Korneliussen and Jansen, 1976; Bixby, 1981; Riley, 1981; Morrison-Graham, 1983). Rich and Lichtman (1989) have shown that acetylcholine receptors diminish in number directly beneath eliminated axons before any obvious change in the axon. Their data suggest that postsynaptic molecules are required for terminal maintenance. If, as seems likely, some of these postsynaptic molecules are involved in adhesion, their loss would cause a decline in axonal tension in a manner similar to severed neurites, possibly inducing motor axon tension generation and retraction. We have previously reported on a model that can, in principle, explain how changes in the support for axonal tension could regulate the microtubule assembly or disassembly that must accompany elongation and retraction (Buxbaum and Heidemann, 1988). This interpretation of the symmetry of the growth and retraction process and its regulation by mechanical force is fundamentally similar to the views of Campenot (1985) and also of George et al. (1988). Particularly striking is the similarity of our conclusions to those of Campenot (1985) in the face of very different experimental regimes for stimulating elongation and retraction. A similar growth regulatory mechanism suggested by studies with applied tension and with a physiological growth factor increases our confidence in the existence of cytomechanical control of neurite length. Finally, the passive viscoelastic response region of Fig. 15 also may have physiological importance in "buffering" this regulatory mechanism from inappropriate signals. In this range, for example, tension changes induced by skeletal movements would not cause elongation or retraction.

We thank Jeff Lichtman for a stimulating conversation and Youyin Choy for technical assistance.

This work was supported by National Science Foundation grant BNS 8807920 and National Institutes of Health grant GM 36894.

Received for publication 21 July 1989 and in revised form 23 August 1989.

References

Baas, P. W., and S. R. Heidemann. 1986. Microtubule reassembly from nucleating fragments during regrowth of amputated neurites. *J. Cell Biol.* 103:917–927.

Bixby, J. L. 1981. Ultrastructural observations of synapse elimination in neonatal rabbit skeletal muscle. *J. Neurocytol.* 10:81–100.

Bray, D. 1982. Filopodial contraction and growth cone guidance. *In* Cell Behavior. R. Bellair, A. Curtis, and G. Dunn, editors. Cambridge University Press, Cambridge. 299–317.

Bray, D. 1984. Axonal growth in response to experimentally applied tension. *Dev. Biol.* 102:379–389.

Bridgman, P. C., and M. E. Dailey. 1989. The organization of myosin and actin in rapid frozen nerve growth cones. *J. Cell Biol.* 108:95–109.

Buxbaum, R. E., and S. R. Heidemann. 1988. A thermodynamic model for force integration and microtubule assembly during axonal elongation. *J. Theor. Biol.* 134:379–390.

Campenot, R. B. 1985. The regulation of nerve fiber length by intercalated elongation and retraction. *Dev. Brain Res.* 20:149–154.

Cowan, W. M., J. W. Fawcett, D. D. M. O'Leary, and B. B. Stanfield. 1984. Regressive events in neurogenesis. *Science (Wash. DC).* 225:1258–1265.

Dennerll, T. J., H. C. Joshi, V. L. Steel, R. E. Buxbaum, and S. R. Heidemann. 1988. Tension and compression in the cytoskeleton. II. Quantitative measurements. *J. Cell Biol.* 107:665–674.

George, E. B., B. F. Schneider, R. J. Lasek, and M. J. Katz. 1988. Axonal shortening and the mechanism of axonal motility. *Cell Motil. Cytoskeleton.* 9:48–59.

Heidemann, S. R., H. C. Joshi, A. Schechter, J. R. Fletcher, and M. Bothwell. 1985. Synergistic effects of cyclic AMP and nerve growth factor on neurite outgrowth and microtubule stability. *J. Cell Biol.* 100:916–927.

Hiramoto, Y. 1963. Mechanical properties of sea urchin eggs. *Exp. Cell Res.* 32:59–75.

Hiramoto, Y. 1970. Rheological properties of sea urchin eggs. *Biorheology.* 6:201–234.

Hirokawa, N. 1982. Cross-linker system between neurofilaments, microtubules, and membranous organelles in frog axons revealed by the quick-freeze, deep-etching method. *J. Cell Biol.* 94:129–142.

Jacobs, J. R., and J. K. Stevens. 1986. Changes in the organization of the neuritic cytoskeleton during nerve growth factor–activated differentiation of PC12 cells: a serial electron microscopic study of the development and control of neurite shape. *J. Cell Biol.* 103:895–906.

Joshi, H. C., D. Chu, R. E. Buxbaum, and S. R. Heidemann. 1985. Tension and Compression in the cytoskeleton of PC 12 Neurites. *J. Cell Biol.* 101:697–705.

Korneliussen, H., and J. K. S. Jansen. 1976. Morphological aspects of the elimination of polyneural innervation of skeletal muscle fibers in newborn rats. *J. Neurocytol.* 5:591–604.

Kuczmarski, E. R., and J. L. Rosenbaum. 1979. Studies on the organization and localization of actin and myosin in neurons. *J. Cell Biol.* 80:356–371.

Lamoureux, P., R. E. Buxbaum, and S. R. Heidemann. 1989. Direct evidence that growth cones pull. *Nature (Lond.).* 340:159–162.

Letourneau, P. C., and A. H. Ressler. 1984. Inhibition of neurite initiation and growth by taxol. *J. Cell Biol.* 98:1355–1362.

Luckenbill-Edds, L., C. VanHorn, and L. A. Greene. 1979. Fine structure of initial outgrowth of processes induced in a pheochromocytoma cell line by nerve growth factor. *J. Neurocytol.* 8:493–511.

Mitchison, T., and N. Kirschner. 1988. Cytoskeletal dynamics and nerve growth. *Neuron.* 1:761–772.

Mitchison, J. M., and M. M. Swann. 1954. The mechanical properties of the cell surface. I. The cell elastimeter. *J. Exp. Biol.* 31:443–460.

Morrison-Graham, K. 1983. An anatomical and electrophysiological study of synapse elimination at the developing frog neuromuscular junction. *Dev. Biol.* 99:298–311.

Pasternak, C., and E. L. Elson. 1985. Lymphocyte mechanical response triggered by cross-linking surface receptors. *J. Cell Biol.* 100:860–872.

Purves, D., and J. W. Lichtman. 1980. Elimination of synapses in the developing nervous system. *Science (Wash. DC).* 210:153–157.

Purves, D., and J. W. Lichtman. 1985. Principles of Neural Development. Sinauer Associates, Inc., Sunderland, MA. 433 pp.

Rich, M. M., and J. W. Lichtman. 1989. In vivo visualization of pre- and postsynaptic changes during synapse elimination in reinnervated mouse muscle. *J. Neurosci.* 9:1781–1805.

Riley, D. A. 1981. Ultrastructural evidence for axon retraction during spontaneous elimination of polyneural innervation of the rat soleus muscle. *J. Neurocytol.* 10:425–440.

Roisen, F., M. Inczedy-Marcsek, L. Hsu, and W. Yorke. 1978. Myosin: immunofluorescent localization in neuronal and glial cultures. *Science (Wash. DC).* 199:1445–1448.

Schiff, P. B., J. Fant, and S. B. Horwitz. 1979. Promotion of microtubule assembly in vitro by taxol. *Nature (Lond.).* 277:665–667.

Schnapp, B. J., and T. S. Reese. 1982. Cytoplasmic structure in rapid frozen axons. *J. Cell Biol.* 94:667–679.

Shaw, G., and D. Bray. 1977. Movement and extension of isolated growth cones. *Exp. Cell Res.* 104:55–62.

Sinclair, G. I., P. W. Baas, and S. R. Heidemann. 1988. Role of microtubules in the cytoplasmic compartmentation of neurons. II. Endocytosis in the growth cone and neurite shaft. *Brain Res.* 450:60–68.

Weiss, P. 1941. Nerve Pattern: The mechanics of nerve growth. *Growth.* 5(Suppl. Third Growth Symp.):163–203.

Wessells, N. K., S. R. Johnson, and R. P. Nuttall. 1978. Axon initiation and growth cone regeneration in cultured motor neurons. *Exp. Cell Res.* 117:335–345.